Eliashberg theory in the weak-coupling limit

F. Marsiglio
Department of Physics, University of Alberta, Edmonton, Alberta, Canada T6G 2E1

(Received 28 June 2018; published 30 July 2018)

Eliashberg theory provides a theoretical framework for understanding the phenomenon of superconductivity when pairing between two electrons is mediated by phonons and retardation effects are fully accounted for. BCS theory is often viewed as the weak-coupling limit of Eliashberg theory, in spite of a handful of papers that have pointed out that this is not so. Here, we present very accurate numerical solutions in the weak-coupling limit to complement the existing analytical results and demonstrate more convincingly the validity of this limit by extending the analytical results to first order in the coupling constant.

DOI: 10.1103/PhysRevB.98.024523

I. INTRODUCTION

The Eliashberg theory of superconductivity [1] provides a framework for superconductivity in which the pairing "glue," in this case phonons, is not so much a "glue" as a mediator of the interaction between two electrons. In contrast, the BCS theory of superconductivity [2] uses a pairing potential to model the attractive interaction between two electrons. Being a potential, the interaction is instantaneous, although retardation effects are mimicked through a cutoff in the potential, albeit in wave-vector space and not in frequency space.

Eliashberg theory is sometimes referred to as the "strong-coupling" extension of BCS theory. The reason no doubt is that superconducting materials in which retardation effects play a significant role (e.g., Pb and Hg) also tend to have a stronger electron-phonon coupling than those in which their role is minor (e.g., Al). Furthermore, in Eliashberg theory the quasiparticles have a finite width, and their residue is no longer unity; both of these factors contributed to this misnomer. In fact, both Eliashberg and BCS theory are weak-coupling theories in the sense that the starting point is a Fermi sea of electrons, so what really delineates the two is that the former explicitly includes retardation effects while the latter does not. Formally, the strong-coupling limit in both these theories can be investigated (and has been; see Refs. [3,4] for BCS and Refs. [5,6] for Eliashberg theory). However, particularly at finite temperature these calculations are beyond the limit of validity of the formulation, as the condensation of preformed pairs, whose constituents *do not* form a Fermi sea, is the physically relevant process but is not described by these theoretical frameworks [7].

There is a tacit understanding that the weak-coupling limits of both theories converge to the same limits. This belief has been reinforced, for example, in studies of universal BCS constants like the gap ratio [8] and the normalized specific-heat jump [9]. In these and other cases [10] the universal BCS constant shows deviations within Eliashberg theory that eventually achieve the BCS value as the coupling becomes weaker.

That this is *not universally* the case was first noted by Karakozov *et al.* [11]. In fact, they showed that a correction to the BCS prefactor appears in the weak-coupling limit of Eliashberg theory for the determination of T_c, the superconducting critical temperature itself. This is an important observation and merits further investigation. In this paper we will rederive this result for T_c (on the imaginary axis, following Ref. [12]), and we will also derive an improved analytical form for the order parameter. Remarkably, the order parameter is not at all a constant over a frequency range of the typical phonon frequency, as modeled both in BCS theory and even in Eliashberg theory with the so-called square-well model for the electron-phonon interaction introduced by McMillan [13].

Note that in this study we examine corrections to BCS that arise entirely within Eliashberg theory; there are a number of additional contributions that have an effect on the prefactor, for example, that of Kohn and Luttinger [14,15], but we do not address those here.

We proceed as follows. First, we provide a quick synopsis of Eliashberg theory. We take some effort to review the so-called standard approximations to arrive at the self-consistent equations for the order parameter as a function of only Matsubara frequency. As emphasized in Ref. [16], these approximations are very controlled particularly in the weak-coupling limit and have properly been avoided or modified for further more recent refinements in the theory [17]. Here, however, these approximations rest on solid ground. We then present both numerical and analytical solutions to the gap function, first following Wang and Chubukov [12] in the case where renormalization effects are neglected and then in the case where they are accounted for. While T_c is unaffected (except for the usual mass renormalization term, $1+\lambda$), the high-frequency dependence of the gap function to first order in λ is indeed changed, as described in more detail below. We conclude with a summary in the final section.

II. ELIASHBERG THEORY FORMALISM

The Eliashberg equations are [18]

$$Z(\mathbf{k}, i\omega_m) = 1 + \frac{1}{N\beta}\sum_{\mathbf{k}',m'} \frac{\lambda_{\mathbf{k}\mathbf{k}'}(i\omega_m - i\omega_{m'})}{g_{\epsilon_F}} \frac{(\omega_{m'}/\omega_m)Z(\mathbf{k}', i\omega_{m'})}{\omega_{m'}^2 Z^2(\mathbf{k}', i\omega_{m'}) + [\epsilon_{\mathbf{k}'} - \mu + \chi(\mathbf{k}', i\omega_{m'})]^2 + \phi^2(\mathbf{k}', i\omega_{m'})}, \tag{1}$$

$$\chi(\mathbf{k}, i\omega_m) = -\frac{1}{N\beta}\sum_{\mathbf{k}',m'} \frac{\lambda_{\mathbf{k}\mathbf{k}'}(i\omega_m - i\omega_{m'})}{g_{\epsilon_F}} \frac{\epsilon_{\mathbf{k}'} - \mu + \chi(\mathbf{k}', i\omega_{m'})}{\omega_{m'}^2 Z^2(\mathbf{k}', i\omega_{m'}) + [\epsilon_{\mathbf{k}'} - \mu + \chi(\mathbf{k}', i\omega_{m'})]^2 + \phi^2(\mathbf{k}', i\omega_{m'})}, \tag{2}$$

along with the equation for the order parameter,

$$\phi(\mathbf{k}, i\omega_m) = \frac{1}{N\beta}\sum_{\mathbf{k}',m'} \frac{\lambda_{\mathbf{k}\mathbf{k}'}(i\omega_m - i\omega_{m'})}{g_{\epsilon_F}} \frac{\phi(\mathbf{k}', i\omega_{m'})}{\omega_{m'}^2 Z^2(\mathbf{k}', i\omega_{m'}) + [\epsilon_{\mathbf{k}'} - \mu + \chi(\mathbf{k}', i\omega_{m'})]^2 + \phi^2(\mathbf{k}', i\omega_{m'})}. \tag{3}$$

These are supplemented with the electron number equation, which determines the chemical potential, μ:

$$\rho = 1 - \frac{2}{N\beta}\sum_{\mathbf{k}',m'} \frac{\epsilon_{\mathbf{k}'} - \mu + \chi(\mathbf{k}', i\omega_{m'})}{\omega_{m'}^2 Z^2(\mathbf{k}', i\omega_{m'}) + [\epsilon_{\mathbf{k}'} - \mu + \chi(\mathbf{k}', i\omega_{m'})]^2 + \phi^2(\mathbf{k}', i\omega_{m'})}. \tag{4}$$

Here, N is the number of lattice sites; $\beta \equiv 1/(k_B T)$, where k_B is the Boltzmann constant and T is the temperature; μ is the chemical potential; and g_{ϵ_F} is the electronic density of states at the Fermi level in the band. The energy $\epsilon_{\mathbf{k}}$ is the electronic dispersion of this band (a single band is assumed for simplicity). The equations are written on the imaginary frequency axis and are functions of the Fermion Matsubara frequencies, $\omega_m \equiv \pi k_B T(2m-1)$, with m being an integer. Similarly, the Boson Matsubara frequencies are given by $\nu_n \equiv 2\pi k_B T n$, where n is an integer. The functions $Z(\mathbf{k}, i\omega_m)$ and $\chi(\mathbf{k}, i\omega_m)$ are related to the electron self-energy through [16]

$$i\omega_m[1 - Z(\mathbf{k}, i\omega_m)] \equiv \tfrac{1}{2}[\Sigma(\mathbf{k}, i\omega_m) - \Sigma(\mathbf{k}, -i\omega_m)],$$
$$\chi(\mathbf{k}, i\omega_m) \equiv \tfrac{1}{2}[\Sigma(\mathbf{k}, i\omega_m) + \Sigma(\mathbf{k}, -i\omega_m)], \tag{5}$$

where Z and χ are both even functions of $i\omega_m$ (and, as we have assumed from the beginning, $\mathbf{k}$). The function $\phi(\mathbf{k}, i\omega_m)$ is the so-called pairing function and is related to the electronic anomalous Green's function. These equations relate these three functions to one another through the electron-phonon propagator, contained in

$$\lambda_{\mathbf{k}\mathbf{k}'}(z) \equiv \int_0^\infty \frac{2\nu\alpha^2_{\mathbf{k}\mathbf{k}'}F(\nu)}{\nu^2 - z^2} d\nu, \tag{6}$$

with $\alpha^2_{\mathbf{k}\mathbf{k}'}F(\nu)$ being the so-called Eliashberg function. In what follows we will assume that the phonon spectrum is given by an Einstein spectrum and that the coupling is wave vector independent. Therefore,

$$\alpha^2_{\mathbf{k}\mathbf{k}'}F(\nu) = (\lambda\omega_E/2)\delta(\nu - \omega_E), \tag{7}$$

and the kernel, Eq. (6), is written as

$$\lambda(i\nu_n) = \frac{\lambda\omega_E^2}{\omega_E^2 + \nu_n^2}, \tag{8}$$

where the constant λ is the dimensionless electron-phonon coupling constant and ω_E is the Einstein phonon frequency. Normally, a direct Coulomb repulsion is also included in the pairing equation; we omit that here since we want to focus on the effects of retardation. Equation (4) is used to determine the chemical potential given an electron density ρ, but in this work we will assume particle-hole symmetry; then $\mu = 0$ always, and this equation is not used, with ρ no longer being relevant. Similarly, $\chi(\mathbf{k}, i\omega_m)$ is identically zero. We furthermore assume that the electronic density of states is essentially a constant over the energy range of interest and set it equal to the value of the density of states at the Fermi level, $g(\mu) \approx g_{\epsilon_F}$. With these assumptions the equations simplify considerably, and none of the functions have any wave vector dependence; that is, they are solely functions of Matsubara frequency ω_m. Focusing our attention on the onset of superconductivity and the critical temperature, we linearize the equations and obtain

$$Z(i\omega_m) = 1 + \frac{\pi T_c}{\omega_m}\sum_{m'} \lambda(i\omega_m - i\omega_{m'})\mathrm{sgn}(\omega_{m'}), \tag{9}$$

$$\phi(i\omega_m) = \pi T_c \sum_{m'} \lambda(i\omega_m - i\omega_{m'}) \frac{\phi(i\omega_{m'})}{|\omega_{m'}|Z(i\omega_{m'})}. \tag{10}$$

The case of a constant density of states but with a finite bandwidth was examined in Ref. [19]; it is apparent from that work that in the weak-coupling limit this bandwidth is irrelevant for T_c [20]. Equations (9) and (10) are the "standard" linearized Eliashberg equations, valid for infinite electronic bandwidth. The function $Z(i\omega_m)$ can be determined in closed form; we obtain, for $\omega_m > 0$ (since both Z and ϕ are even real functions of ω_m),

$$Z(i\omega_m) = 1 + \frac{\pi k_B T_c}{\omega_m}\left\{\lambda + 2\sum_{n=1}^{m-1}\lambda(i\nu_n)\right\}. \tag{11}$$

It is also standard practice to define a "gap function," $\Delta(i\omega_m) \equiv \phi(i\omega_m)/Z(i\omega_m)$, so that the remaining equation to determine T_c is

$$Z(i\omega_m)\Delta(i\omega_m) = \pi T_c \sum_{m'=-\infty}^{+\infty} \lambda(i\omega_m - i\omega_{m'}) \frac{\Delta(i\omega_{m'})}{|\omega_{m'}|}. \tag{12}$$

Equations (11) and (12) were first solved in this form in Refs. [21–23] and have been solved many times since.

As mentioned in the Introduction, one can examine Eliashberg theory in limiting cases of weak coupling ($\lambda \to 0$) and strong coupling $\lambda \to \infty$. Interestingly, Eq. (12) is readily solved numerically in the latter limit (see, e.g., Refs. [5,6,24]) but not so easily in the former limit. Approximate forms like the square-well model were first used by McMillan [13] and adopted in subsequent reviews [16,18]. In the end, however, McMillan and others adopted phenomenological prefactors, whose justification is now more readily understood after Karakozov *et al.* [25] solved the gap equation on the real axis with an iterative method and obtained the result that T_c attains a prefactor significantly different than that obtained with BCS theory [26]. We will first rederive this result on the imaginary axis [12] and determine an analytical approximation for the gap function.

The equation for T_c within BCS theory is (we now set $k_B = 1$ and $\hbar = 1$)

$$T_c = 1.13\omega_E \exp(-1/\lambda), \tag{13}$$

where $\lambda \equiv g_{\epsilon_F}|V|$, with $|V|$ being some attractive and instantaneous potential between two electrons. The inclusion of the renormalization Z modifies this equation to read

$$T_c = 1.13\omega_E \exp[-(1+\lambda)/\lambda]. \tag{14}$$

One can immediately write this like Eq. (13) but with the reduced prefactor $1.13e^{-1}$. This is *not* what is meant when we stated that the prefactor in Eliashberg theory is actually modified from the BCS result, but rather an additional change occurs.

III. UNRENORMALIZED ELIASHBERG THEORY

A. Improved T_c in the $\lambda \to 0$ limit

To emphasize the latter point we first examine the Eliashberg T_c equation, Eq. (12) with $Z(i\omega_m) \equiv 1$, i.e.,

$$\Delta(i\omega_m) = \pi T_c \sum_{m'=-\infty}^{+\infty} \lambda(i\omega_m - i\omega_{m'}) \frac{\Delta(i\omega_{m'})}{|\omega_{m'}|}. \tag{15}$$

We immediately caution that this is a dangerous step to make, as emphasized by Cappelluti and Ummarino [27]. In fact, this choice results in unstable equations for $\lambda > 1$. Since we are interested only in the weak-coupling limit $\lambda \ll 1$, Eq. (15) remains stable. In what follows we make use of the fact that even within Eliashberg theory the structure of Eq. (13) remains intact, so that $T_c/\omega_E \approx e^{-1/\lambda} \ll 1$ for the weak-coupling case. The impact on $\Delta(\omega_m)$ is, however, a little more subtle, and a discussion of this case will be deferred to the next section.

For now, with $Z(\omega_m) = 1$, we begin by writing Eq. (15) as

$$\begin{aligned}\Delta(i\omega_m) &= \lambda\pi\bar{T}_c \sum_{m'=-\infty}^{+\infty} \frac{1}{1+(\bar{\omega}_m - \bar{\omega}_{m'})^2} \frac{\Delta(i\omega_{m'})}{|\bar{\omega}_{m'}|} \qquad (16)\\ &= \frac{1}{1+\bar{\omega}_m^2} \lambda\pi\bar{T}_c \sum_{m'=-\infty}^{+\infty} \left\{1 + \frac{2\bar{\omega}_m\bar{\omega}_{m'} - \bar{\omega}_{m'}^2}{1+(\bar{\omega}_m - \bar{\omega}_{m'})^2}\right\} \frac{\Delta(i\omega_{m'})}{|\bar{\omega}_{m'}|}, \qquad (17)\end{aligned}$$

where $\bar{Q} \equiv Q/\omega_E$, and in the second line we have added and subtracted the factor $1/(1+\bar{\omega}_m^2)$. Equation (17) makes it clear that one can write

$$\Delta(i\omega_m) = \frac{1}{1+\bar{\omega}_m^2}[1 + \lambda f(\omega_m)]. \tag{18}$$

This equation looks like a perturbative expansion in λ; if we neglect $f(\omega_m)$ and *further* neglect the second complicated-looking term in Eq. (17), we obtain simply

$$1 \approx \lambda\pi\bar{T}_c \sum_{m'=-\infty}^{+\infty} \frac{1}{|\bar{\omega}_{m'}|} \frac{1}{1+\bar{\omega}_{m'}^2} \equiv \lambda I_0, \tag{19}$$

where I_0 can be evaluated in terms of the asymptotic expansion of digamma functions [28,29] as

$$I_0 \approx \ln\left(\frac{1.13\omega_E}{T_c}\right) - \frac{\pi^2}{6}\left(\frac{T_c}{\omega_E}\right)^2. \tag{20}$$

Upon neglecting the last term, the result is that we obtain the usual BCS T_c equation given by Eq. (13). In fact, it is inconsistent to neglect the complicated-looking second term in Eq. (17). Thus, while still neglecting the corrections proportional to $f(\omega_m)$, a more accurate version of Eq. (19) more correctly contains an additional term, so this equation reads

$$1 \approx \lambda I_0 + \lambda\pi\bar{T}_c \sum_{m'=-\infty}^{+\infty} \frac{1}{1+\bar{\omega}_{m'}^2} \frac{2\bar{\omega}_m \mathrm{sgn}(\bar{\omega}_{m'}) - |\bar{\omega}_{m'}|}{1+(\bar{\omega}_m - \bar{\omega}_{m'})^2}. \tag{21}$$

This equation is clearly an approximation since the second term has a dependence on ω_m; this reflects the approximation inherent in Eq. (18) when $f(\omega_m)$ is neglected. Nonetheless, we multiply both sides of Eq. (21) by $\pi\bar{T}_c\{1/|\bar{\omega}_m|\}\{1/(1+\bar{\omega}_m^2)\}$ and sum over all values of m to obtain

$$\begin{aligned}I_0 = \lambda I_0^2 - \lambda(\pi\bar{T}_c)^2 \sum_{m,m'=-\infty}^{+\infty} &\frac{1}{1+\bar{\omega}_{m'}^2} \frac{1}{|\bar{\omega}_m|} \frac{1}{1+\bar{\omega}_m^2}\\ &\times \left\{\frac{|\bar{\omega}_{m'}| - 2\bar{\omega}_m \mathrm{sgn}(\bar{\omega}_{m'})}{1+(\bar{\omega}_m - \bar{\omega}_{m'})^2}\right\}. \end{aligned} \tag{22}$$

We use [12]

$$\begin{aligned}&\frac{1}{1+(\bar{\omega}_m - \bar{\omega}_{m'})^2}\\ &\quad = \frac{1}{1+\bar{\omega}_{m'}^2} + \left\{\frac{1}{1+(\bar{\omega}_m - \bar{\omega}_{m'})^2} - \frac{1}{1+\bar{\omega}_{m'}^2}\right\} \end{aligned} \tag{23}$$

to replace the term in braces in Eq. (22). The first term (proportional to $|\bar{\omega}_{m'}|$ in the numerator of the sum) in this equation is seen to contain a singular part as $T_c \to 0$ (since a denominator proportional to $|\bar{\omega}_m|$ remains), which in effect offsets the diminution of λ in the prefactor. The singular part is extracted by adding and subtracting $\{1/(1+\bar{\omega}_{m'}^2)\}$ as indicated in Eq. (23). Then the first term contains the singular part, while the remainder is of order unity and therefore remains small due to the λ prefactor. Equation (22) then becomes

$$I_0 = \lambda I_0^2 - I_0/2, \tag{24}$$

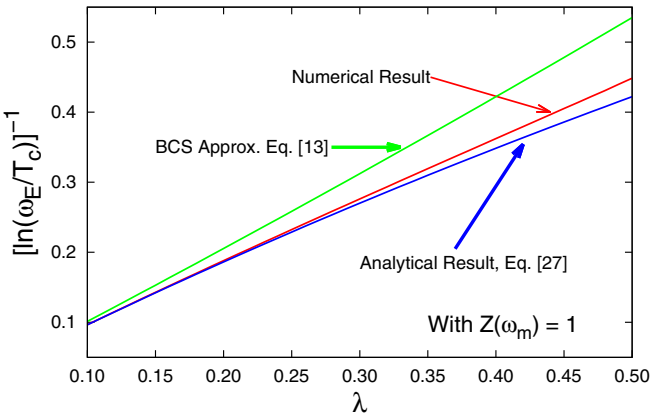

FIG. 1. A plot of $[\ln(\omega_E/T_c)]^{-1}$ vs λ. Numerical results are shown in red; the usual BCS approximation, Eq. (13), is given by the green curve, while the improved estimate given by Eq. (26) is shown in blue. This latter result becomes essentially exact for $\lambda \lessapprox 0.2$.

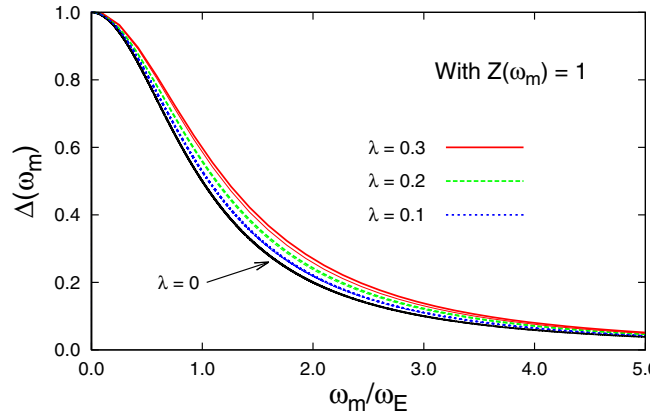

FIG. 2. A plot of $\Delta(\omega_m)$ vs $\bar{\omega}_m \equiv \omega_m/\omega_E$ for $\lambda = 0.3$, 0.2, and 0.1 as indicated, obtained numerically. Also shown is the approximation given by Eq. (18) with $f(\omega_m) = 0$. It is clear that deviations from this limiting result certainly exist, but the numerical results are trending towards this weak-coupling result. Note that all curves shown are actually a discrete set of points, determined at the Matsubara frequencies, but curves have been drawn for better presentation. In reality only the results for $\lambda = 0.3$ are readily discerned as a discrete set. For reference, the two-square-well model would be a step function with a value of unity for $0 < \bar{\omega}_m < 1$ and a value of zero beyond. The numerical values of T_c/ω_E for each of these cases is $T_c/\omega_E = 0.026744(\lambda = 0.3)$, $0.004900(\lambda = 0.2)$, and $0.000032(\lambda = 0.1)$. Note that an improved approximation to first order in λ, given by Eq. (33) with $g_1(\omega_m)$ provided by Eq. (32), is shown with a thin curve of the same color for each value of λ. The result is discernible from the numerical result only in the case of $\lambda = 0.3$.

where we have used the fact that

$$I_4 \equiv (\pi \bar{T}_c) \sum_{m=-\infty}^{+\infty} \frac{|\bar{\omega}_m|}{\left(1+\bar{\omega}_m^2\right)^2} \approx \frac{1}{2}. \tag{25}$$

Following Refs. [11,12] we solve Eq. (24) to obtain

$$T_c = \frac{1.13}{\sqrt{e}} \omega_E \exp\left(-1/\lambda\right), \tag{26}$$

in contrast to Eq. (13).

Figure 1 shows results from unrenormalized Eliashberg theory (solved numerically), along with the BCS result from Eq. (13) and the improved result from Eq. (26). In particular we plot $[\ln(\omega_E/T_c)]^{-1}$ vs λ. The numerical results are given as a red curve as indicated, while the BCS approximation (13) and the improved result from Eq. (26) are given by green and blue curves, respectively, as indicated. It is clear that the improved result is essentially exact for the weakest electron-phonon couplings shown.

B. Improved gap function in the $\lambda \to 0$ limit

One of the physical features of the square-well model referred to in the previous section is that the gap function is a constant for a range of energies equal to the phonon frequency (here, ω_E) on either side of the Fermi energy. This is already not true with the approximation provided by Eq. (18), even with neglecting $f(\omega_m)$. In Fig. 2 we show with thick curves the numerical result for the gap function for several weak values of the coupling parameter λ, along with the result from Eq. (18) with $f(\omega_m) \equiv 0$. This latter result, with $f(\omega_m) = 0$, is independent of λ and will presumably be correct in the strict $\lambda \to 0$ limit. Figure 2 clearly confirms that the numerical results are indeed trending towards this result.

In an effort to further improve this result and refine our understanding of the weak-coupling limit, we proceed to determine $f(\omega_m)$ at least as a correction to zeroth order in λ (and thus an overall correction to the gap function to first order in λ). For this purpose we substitute Eq. (18) into Eq. (17); upon isolating $f(\omega_m)$ we obtain

$$f(\omega_m) = c - g_1(\omega_m) - \lambda g_2(\omega_m), \tag{27}$$

where c is a constant given by

$$c = -\frac{1}{\lambda} + I_0 + \lambda \pi \bar{T}_c \sum_{m'=-\infty}^{+\infty} \frac{f(\omega_{m'})}{|\bar{\omega}_{m'}|} \frac{1}{1+\bar{\omega}_{m'}^2}, \tag{28}$$

and

$$g_1(\omega_m) = \pi \bar{T}_c \sum_{m'=-\infty}^{+\infty} \frac{1}{1+\bar{\omega}_{m'}^2} \left\{ \frac{|\bar{\omega}_{m'}| - 2\bar{\omega}_m \mathrm{sgn}(\bar{\omega}_{m'})}{1+(\bar{\omega}_m - \bar{\omega}_{m'})^2} \right\} \tag{29}$$

and

$$g_2(\omega_m) = \pi \bar{T}_c \sum_{m'=-\infty}^{+\infty} \frac{f(\omega_{m'})}{1+\bar{\omega}_{m'}^2} \left\{ \frac{|\bar{\omega}_{m'}| - 2\bar{\omega}_m \mathrm{sgn}(\bar{\omega}_{m'})}{1+(\bar{\omega}_m - \bar{\omega}_{m'})^2} \right\} \tag{30}$$

are two functions of ω_m. Both $g_1(\omega_m)$ and $g_2(\omega_m)$ are non-singular as $\lambda \to 0$. By this we mean that a $1/|\bar{\omega}_{m'}|$ term is absent [as opposed to I_0, for example, the sum multiplying λ in Eq. (19)]; this means both of these functions are of order unity. Since λ premultiplies $g_2(\omega_m)$, g_2 can be ignored, bearing in mind we wish to retain terms in $f(\omega_m)$ of order unity or better.

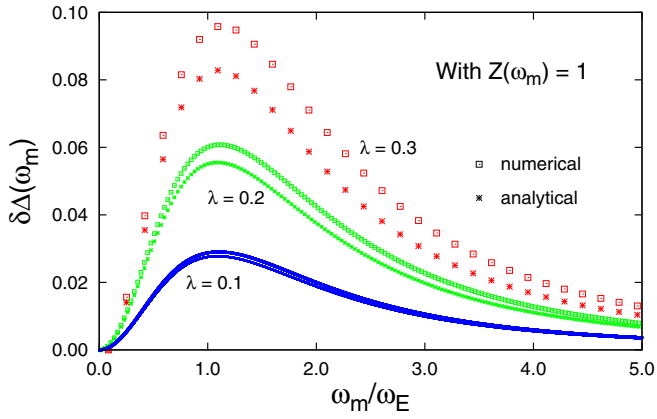

FIG. 3. A plot of the deviation from $\Delta_0(\omega_m)$ [see Eq. (34)] given by the numerical results (shown with squares) and by the analytical results (shown with asterisks) for the three different values of λ indicated and through the color scheme. In all cases the first-order correction to the gap function obtained analytically through Eq. (32) very accurately accounts for the discrepancy from $\Delta_0(\omega_m)$, which was not discernible in Fig. 2. Note that for the two lowest values of λ only a subset of the Matsubara frequencies was used; otherwise, the results would have appeared as a continuous curve.

The resulting expression for the constant c is

$$c = -\frac{1}{\lambda} + I_0 + \lambda c I_0 - \lambda\left(\frac{1}{2}I_0 + c'\right), \tag{31}$$

where c' is a constant obtained numerically from the sum in Eq. (28) with $g_1(\omega_m)$ substituted as part of $f(\omega_m)$. In any event c' is irrelevant as it is multiplied by λ and enters only at higher order in λ. The result is $c = 1/2$, obtained already through the eigenvalue equation, Eq. (24). This results in an improved T_c result given by Eq. (26).

This leaves the explicit expression for $g_1(\omega_m)$ in Eq. (29); this can be evaluated to order $(T_c/\omega_E)^2$ through the properties of digamma functions [28,29],

$$g_1(\omega_m) = \frac{1}{4+\bar{\omega}_m^2}\left\{\frac{2-\bar{\omega}_m^2}{\bar{\omega}_m}\tan^{-1}\bar{\omega}_m - \frac{3}{2}\ln\left(1+\bar{\omega}_m^2\right)\right\}, \tag{32}$$

and we now have a more accurate explicit expression for the gap function,

$$\Delta(\omega_m) = \frac{1}{1+\bar{\omega}_m^2}\left\{1+\lambda\left[\frac{1}{2} - g_1(\omega_m)\right]\right\}, \tag{33}$$

valid to order λ. Three thin curves showing this result for $\lambda = 0.1, 0.2$, and 0.3 on the scale of Fig. 2 are essentially indistinguishable from the numerical results and show that up to $\lambda \approx 0.3$ at least, Eq. (33), with $g_1(\omega_m)$ from Eq. (32), is very accurate for small but nonzero values of λ.

To better appreciate the remaining discrepancies, we show in Fig. 3 results for the deviation from the universal result,

$$\Delta_0(\omega_m) = \frac{1}{1+\bar{\omega}_m^2}, \tag{34}$$

defined as $\delta\Delta_{\rm num}(\omega_m) \equiv \Delta_{\rm num}(\omega_m) - \Delta_0(\omega_m)$, where $\Delta_{\rm num}(\omega_m)$ refers to the numerical solution [30] and $\delta\Delta_{\rm ana}(\omega_m) \equiv \Delta_{\rm ana}(\omega_m) - \Delta_0(\omega_m)$, where $\Delta_{\rm ana}(\omega_m)$ refers to the analytical solution given by Eq. (33). The remaining discrepancies for the gap function are of order λ^2. At this point we return to the theory with $Z(\omega_m) \neq 1$ and indicate the places where the description differs from the one just provided.

IV. ELIASHBERG THEORY WITH RENORMALIZATION

In this section we provide solutions for Eq. (12), while accounting for Eq. (11). The numerical procedure is fairly straightforward and follows what we did earlier. A noteworthy nuance is that the $m = m'$ term on the right side of Eq. (12) no longer contributes; it is precisely canceled by a term on the left that arises upon substituting Eq. (11) into Eq. (12), and this is a manifestation of the lack of effect of impurities on superconducting T_c, a fact pointed out by Anderson in Ref. [31]. In any event this is properly accounted for in both the numerical and analytical results and manifests itself not just in T_c but also in the actual functional dependence of the gap function, as we shall see below.

The difference from the previous section is that $Z(\omega_m)$ is now included. The sum in Eq. (9) is readily evaluated in terms of digamma functions [28,29]. Omitting terms of order T_c/ω_E, we readily obtain

$$Z(\omega_m) \approx 1 + \lambda\frac{1}{\bar{\omega}_m}\tan^{-1}\bar{\omega}_m, \tag{35}$$

which interpolates smoothly from $(1+\lambda)$ at low frequencies to unity at high frequencies. Including this in the steps leading to Eq. (18), we obtain here instead

$$\Delta(\omega_m) = \frac{1}{1+\bar{\omega}_m^2}\left\{1+\lambda\left[f_Z(\omega_m) - \frac{1}{|\bar{\omega}_m|}\tan^{-1}|\bar{\omega}_m|\right]\right\}. \tag{36}$$

Following the same type of analysis as that leading to Eq. (26) and to Eq. (33), we find here that

$$T_c = \frac{1.13}{\sqrt{e}}\omega_E \exp\left[-(1+\lambda)/\lambda\right] \tag{37}$$

and

$$f_Z(\omega_m) = \tfrac{3}{2} - g_1(\omega_m), \tag{38}$$

where $g_1(\omega_m)$ is the same function as that given in Eq. (32). As previously mentioned, Eq. (37) can, of course, be written with $-1/\lambda$ in the exponential, along with a prefactor denominator of $e^{3/2}$ instead of $\sqrt{e}$. However, the present form more explicitly shows the role of the "normal-state" renormalization that gives rise to the usual $1+\lambda$ factor, *along* with the not-so-usual $\sqrt{e}$ denominator in the prefactor.

Written out explicitly, Eq. (36) reads

$$\Delta(\omega_m) = \frac{1}{1+\bar{\omega}_m^2}\left(1+\lambda\left[\frac{3}{2} - \frac{1}{4+\bar{\omega}_m^2}\left\{\frac{2-\bar{\omega}_m^2}{\bar{\omega}_m}\tan^{-1}\bar{\omega}_m - \frac{3}{2}\ln(1+\bar{\omega}_m^2)\right\} - \frac{1}{|\bar{\omega}_m|}\tan^{-1}|\bar{\omega}_m|\right]\right). \tag{39}$$

While Eq. (39) looks very much like Eq. (33) with $3/2$ vs $1/2$ to account for the $1+\lambda$ renormalization, there is one important difference: the large ω_m dependence of the first-order

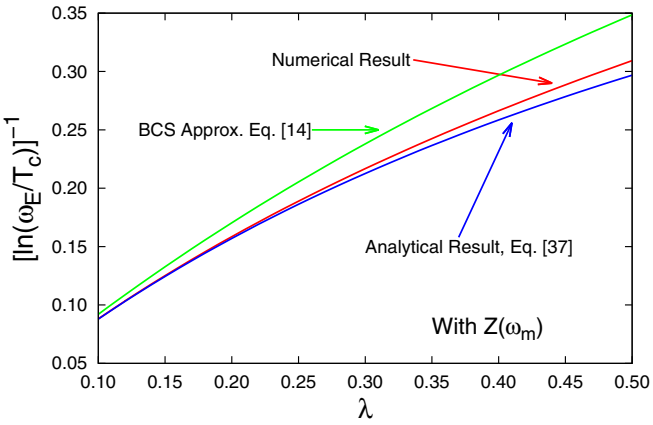

FIG. 4. A plot of $[\ln(\omega_E/T_c)]^{-1}$ vs λ for the case where the normal-state renormalization provided by $Z(\omega_m)$ is accounted for. Numerical results are shown in red; the usual BCS approximation, Eq. (14), is given by the green curve, while the improved estimate given by Eq. (37) is shown in blue. This latter result becomes essentially exact for $\lambda \lessapprox 0.2$, and the improvement is similar to that obtained in Fig. 1.

term in λ is now $\approx (1/\omega_m^2)$ rather than $\approx (1/|\omega_m|)$, as was the case with $Z(\omega_m) = 1$. Figures 4, 5, and 6 essentially repeat the results of Figs. 1, 2 and 3, respectively, now with $Z(\omega_m) \neq 1$. Figure 4 shows at these small values of λ the

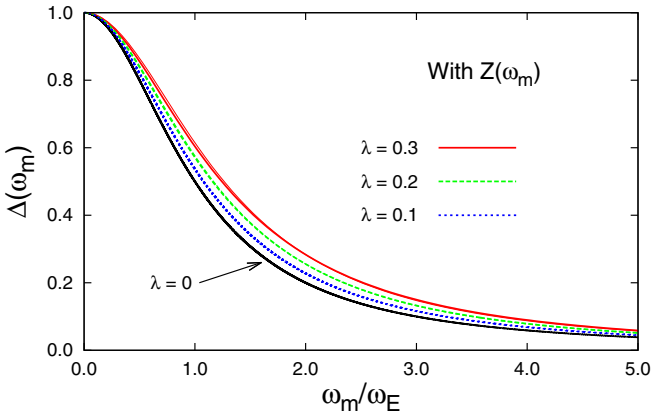

FIG. 5. Similar to Fig. 2, a plot of $\Delta(\omega_m)$ vs $\bar{\omega}_m \equiv \omega_m/\omega_E$ for $\lambda = 0.3, 0.2$, and 0.1 as indicated, obtained numerically (thick curves), now with the full expression for $Z(\omega_m)$ included. Also shown is the $\lambda \to 0$ approximation given by $1/(1+\bar{\omega}_m^2)$ as in Fig. 2. As in that case, deviations from this limiting result are apparent, but the numerical results are certainly trending towards this weak-coupling result. Note that all curves shown are actually a discrete set of points, determined at the Matsubara frequencies, but continuous curves have been drawn for better presentation. In reality only the results for $\lambda = 0.3$ are readily discerned as a discrete set. In this case also, the two-square-well model would be a step function with a value of unity for $0 < \bar{\omega}_m < 1$ and a value of zero beyond. The numerical values of T_c/ω_E for each of these cases is $T_c/\omega_E = 0.009923(\lambda = 0.3)$, $0.001821(\lambda = 0.2)$, and $0.000012(\lambda = 0.1)$. Note that an improved approximation to first order in λ, given by Eq. (39), is shown with a thin curve of the same color for each value of λ. The result is again barely discernible from the numerical result only in the case of $\lambda = 0.3$.

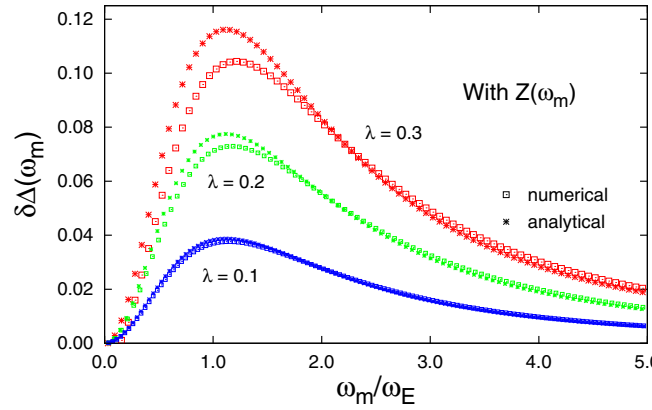

FIG. 6. Similar to Fig. 3, a plot of the deviation from $\Delta_0(\omega_m)$ [see Eq. (34)] given by the numerical results (shown with squares) and by the analytical results (shown with asterisks) for the three different values of λ indicated and through the color scheme. In all cases the first-order correction to the gap function obtained analytically through Eq. (32) very accurately accounts for the discrepancy from $\Delta_0(\omega_m)$; this discrepancy was not so discernible in Fig. 5. Note that for the two lowest values of λ only a subset of the Matsubara frequencies was used; otherwise, the results would have appeared as a continuous curve.

detrimental effect of increased electron-phonon coupling that arises through the normal scattering processes included in the normal part of the self-energy [included when $Z(\omega_m)$ is not equal to unity]; this is apparent in the negative curvature of T_c as a function of λ. In Fig. 5, where the gap function is plotted as a function of Matsubara frequency, the results look qualitatively very similar to those in Fig. 2. Similarly, in Fig. 6 the deviations from a decaying Lorentzian function look very similar to those in Fig. 3. The analytical results look equally impressive, although in Fig. 6 the extra corrections from the renormalization function $Z(\omega_m)$ are included, and the decay at large frequency (not shown) is the inverse of the square of the Matsubara frequency.

It is worth noting that with the explicit function of the Matsubara frequency given by Eq. (39), an analytical continuation to the real frequency is straightforward. The Lorentzian on the imaginary axis now becomes a square-root singularity on the real axis, with the singularity occurring at the phonon frequency, once again highlighting that the gap function is definitely *not* constant for frequencies up to the Einstein frequency, as in BCS theory. An additional gap structure as a function of frequency will arise in the term proportional to λ, but this structure will, of course, be weak in this limit.

V. SUMMARY

By now extensive solutions have been shown in innumerable papers for the gap function solution to the Eliashberg equations, as indicated in the various reviews cited. In this paper we filled a hole in this tabulation by presenting numerical solutions and analysis in the weak-coupling limit. The difficulty until now has been the number of Matsubara frequencies required for demonstrable convergence. For example, we have used more than 120 000 (positive) Matsubara frequencies to achieve convergence for some of the low electron-phonon couplings

used in this study. We have also obtained analytical solutions to first order in the coupling constant to reinforce these numerical solutions. The main messages of this study, reinforcing those of Refs. [11,12], are as follows:

(i) The weak-coupling expression for superconducting T_c has a reduced prefactor multiplying the phonon frequency scale.

(ii) The gap function approaches a Lorentzian function of frequency as $\lambda \to 0$, and first-order corrections provide very good, quantitatively correct results when compared to numerical results. This corrects the impression that the frequency dependence of the order parameter is a feature that arises in Eliashberg theory *only beyond* the weak-coupling regime. In fact, it remains a characteristic of the superconducting state even in the weak-coupling limit, in contrast to the picture provided in the BCS model calculation.

Further investigation will include results in the superconducting state, below T_c and at zero temperature. In particular, the gap edge at zero temperature, given in BCS theory by an analytical result similar to that of T_c [Eq. (13) or (14)], will also acquire a correction in weak-coupling Eliashberg theory analogous to that for T_c, i.e., Eq. (26) or (37), so that the gap ratio remains universal as $\lambda \to 0$ [8]. Another avenue of possible investigation, perhaps through the Josephson effect, is to determine whether the frequency dependence of the gap function can be measured, even in weakly coupled superconductors like aluminum.

Note added in proof: We were alerted to T_c solutions in the literature after this paper was submitted. In Ref. [34] expressions were derived for T_c in the weak coupling limit for any shape of $\alpha^2 F(\nu)$, while in Ref. [35] the authors use a more general framework that nonetheless reproduces the correct prefactor for T_c in the weak coupling limit. We are grateful to Roland Combescot and Jim Freericks for bringing these papers to our attention.

ACKNOWLEDGMENTS

This work was supported in part by the Natural Sciences and Engineering Research Council of Canada (NSERC). I thank A. Chubukov, who first brought this problem to my attention many years ago and kindly provided me with introductory notes for the derivation of Eq. (26).

[1] G. M. Eliashberg, Interactions between Electrons and Lattice Vibrations in a Superconductor, Zh. Eksp. Teor. Fiz. **38**, 966 (1960) [Sov. Phys. JETP **11**, 696 (1960)].

[2] J. Bardeen, L. N. Cooper, and J. R. Schrieffer, Microscopic theory of superconductivity, Phys. Rev. **106**, 162 (1957); Theory of superconductivity, **108**, 1175 (1957).

[3] D. J. Thouless, Strong-coupling limit in the theory of superconductivity, Phys. Rev. **117**, 1256 (1960).

[4] J. C. Swihart, Solutions of the BCS integral equation and deviations from the law of corresponding states, IBM J. Res. Dev. **6**, 14 (1962).

[5] P. B. Allen and R. C. Dynes, Transition temperature of strong-coupled superconductors reanalyzed, Phys. Rev. B **12**, 905 (1975).

[6] F. Marsiglio and J. P. Carbotte, Gap function and density of states in the strong-coupling limit for an electron-boson system, Phys. Rev. B **43**, 5355 (1991).

[7] Zero-temperature properties, at least for BCS theory, are a different matter, as Leggett [32] first emphasized. He pointed out that the BCS ground state is qualitatively correct even in the strong-coupling limit. Extensions of these ideas were presented in Ref. [33] and have continued to the present.

[8] B. Mitrović, H. G. Zarate, and J. P. Carbotte, The ratio $\frac{2\Delta_0}{k_B T_c}$ within Eliashberg theory, Phys. Rev. B **29**, 184 (1984).

[9] F. Marsiglio and J. P. Carbotte, Strong-coupling corrections to bardeen-cooper-schrieffer ratios, Phys. Rev. B **33**, 6141 (1986).

[10] J. P. Carbotte, Properties of boson-exchange superconductors, Rev. Mod. Phys. **62**, 1027 (1990).

[11] A. E. Karakozov, E. G. Maksimov, and S. A. Mashkov, Effect of the frequency dependence of the electron-phonon interaction spectral function on the thermodynamic properties of superconductors, Zh. Eksp. Teor. Fiz. **68**, 1937 (1975) [Sov. Phys. JETP **41**, 971 (1976)]; O. V. Dolgov, I. I. Mazin, A. A. Golubov, S. Y. Savrasov, and E. G. Maksimov, Critical Temperature and Enhanced Isotope Effect in the Presence of Paramagnons in Phonon-Mediated Superconductors, Phys. Rev. Lett. **95**, 257003 (2005).

[12] Y. Wang and A. Chubukov, Quantum-critical pairing in electron-doped cuprates, Phys. Rev. B **88**, 024516 (2013), Appendix A. We are grateful to A. Chubukov for sharing personal notes detailing this derivation with us.

[13] W. L. McMillan, Transition temperature of strong-coupled superconductors, Phys. Rev. **167**, 331 (1968).

[14] W. Kohn and J. M. Luttinger, New Mechanism for Superconductivity, Phys. Rev. Lett. **15**, 524 (1965); J. M. Luttinger, New mechanism for superconductivity, Phys. Rev. **150**, 202 (1966).

[15] A. Chubukov (private communication). See also Ref. [12] for an implementation of the Kohn-Luttinger calculation in a mechanism proposed for cuprates.

[16] P. B. Allen and B. Mitrović, Theory of Superconducting T_c, Solid State Phys. **37**, 1 (1983).

[17] See, for example, reviews in A. V. Chubukov, D. Pines, and J. Schmalian, A Spin Fluctuation Model for d-Wave Superconductivity, in *Superconductivity, Conventional and Unconventional Superconductors*, edited by K. H. Bennemann and J. B. Ketterson (Springer, Berlin, 2008), pp. 1349–1413; D. Manske, I. Eremin, and K. H. Bennemann, Electronic Theory for Superconductivity in High-T_c Cuprates and Sr_2RuO_4, in *Superconductivity, Conventional and Unconventional Superconductors*, edited by (Springer, Berlin, 2008), pp. 1415–1515.

[18] F. Marsiglio and J. P. Carbotte, Electron-Phonon Superconductivity, in *Superconductivity, Conventional and Unconventional Superconductors*, edited by K. H. Bennemann and J. B. Ketterson (Springer, Berlin, 2008), pp. 73–162.

[19] F. Marsiglio, Eliashberg theory of the critical temperature and isotope effect. dependence on bandwidth, band-filling, and direct coulomb repulsion, J. Low Temp. Phys. **87**, 659 (1992).

[20] While the finite electronic bandwidth is irrelevant for superconducting T_c in the weak-coupling limit, it does remain relevant for other dynamic quantities even in this limit. See F. Doğan and

F. Marsiglio, Self-consistent modification to the electron density of states due to electron-phonon coupling in metals, Phys. Rev. B **68**, 165102 (2003).

[21] C. S. Owen and D. J. Scalapino, S-state instabilities for retarded interactions, Physica (Amsterdam) **55**, 691 (1971).

[22] G. Bergmann and D. Rainer, The sensitivity of the transition temperature to changes in $\alpha^2 F(\omega)$, Z. Phys. **263**, 59 (1973).

[23] D. Rainer and G. Bergmann, Temperature-dependence of H_{c2} and κ_1 in strong coupling superconductors, J. Low Temp. Phys. **14**, 501 (1974).

[24] J. P. Carbotte, F. Marsiglio, and B. Mitrović, Maximum $2\Delta_0/k_B T_c$ for electron-phonon superconductors, Phys. Rev. B **33**, 6135 (1986).

[25] See the un-numbered equation following Eq. (29) in Ref. [11], in particular the first term of $1/2$ for A.

[26] Specifically, instead of the usual prefactor, $1.134 \equiv 2e^{\gamma}/\pi$, where $\gamma \equiv 0.5772\ldots$ is Euler's constant, they obtained $1.134/e^{1/2}$.

[27] E. Cappelluti and G. A. Ummarino, Strong-coupling properties of unbalanced Eliashberg superconductors, Phys. Rev. B **76**, 104522 (2007).

[28] M. Abramowitz and I. A. Stegun, *Handbook of Mathematical Functions* (Dover, New York, 1972).

[29] F. W. J. Olver, D. W. Lozier, R. F. Boisvert, and C. W. Clark, *NIST Handbook of Mathematical Functions* (Cambridge University Press, Cambridge, 2010).

[30] There are some very slight inconsistencies since our numerical solution is always normalized so that $\Delta_{\rm num}(\omega_1) \equiv 1$, but these differences are not discernible on the scale of the plots shown.

[31] P. W. Anderson, Theory of dirty superconductors, J. Phys. Chem. Solids **11**, 26 (1959).

[32] A. J. Leggett, Cooper pairing in spin-polarized Fermi systems, J. Phys. C **7**, 19 (1980); Diatomic Molecules and Cooper Pairs, in *Modern Trends in the Theory of Condensed Matter*, edited by S. Pekalski and J. Przystawa (Springer, Berlin, 1980), p. 13.

[33] P. Nozières and S. Schmitt-Rink, Bose condensation in an attractive fermion gas: From weak to strong coupling superconductivity, J. Low Temp. Phys. **59**, 195 (1985).

[34] R. Combescot, Critical temperature of superconductors: Exact solution from Eliashberg equations on the weak-coupling side, Phys. Rev. B **42**, 7810 (1990).

[35] J. K. Freericks and D. J. Scalapino, Weak-coupling expansions for the attractive Holstein and Hubbard models, Phys. Rev. B **49**, 6368 (1994).